Importance of the model selection for processing dynamic three-point bending tests

Franck Delvare, B. Durand, Jean-Luc Hanus, Sébastien Richomme

HAL Id: ineris-00973604

https://ineris.hal.science/ineris-00973604

Submitted on 4 Apr 2014

IMPORTANCE OF MODEL SELECTION FOR PROCESSING DYNAMIC THREE-POINT BENDING TESTS

F. Delvare[1*], B. Durand[1,2] , J.L. Hanus[1], and S. Richomme[2]

[1]Institut PRISME, Ecole Nationale Supérieure d'Ingénieurs de Bourges
88, Boulevard Lahitolle, 18020 Bourges, FRANCE
Email: bastien.durand,franck.delvare,jean-luc.hanus@ensi-bourges.fr

[2]Institut National de L'Environnement Industriel et des RISques, Unite REST
Parc Technologique ALATA, BP 2, 60550 Verneuil-en-Halatte, FRANCE
Email: sebastien.richomme@ineris.fr

ABSTRACT

The Split-Hopkinson Pressure Bar apparatus remains the standard test to investigate high strain rate materials properties. To determine the tensile strength of quasi-brittle materials three-point bending tests are frequently employed. In this paper, we compare different analytical models for processing the recorded experimental wave signals. It is concluded that only the semi-infinite beam model and the modal superposition analysis with several modes are relevant to get precise strain rate and material dynamic characteristics.

1 INTRODUCTION

Safety analysis of structural systems need to adress a wide range of malevolent attacks or accident scenarios. Due to the extreme nature of blast or impact loadings, the deformation and fracture behaviour of materials differ signif cantly to that observed under quasi-static conditions. Precise rate dependent material characteristics, used as constitutive models parameters, are required to perform accurate numerical simulations of the response of structures to transient loadings. Hopkinson bar experimental techniques have overcomed limitations of conventional servohydraulic testing instrument or drop weight impact test at high strain rates [1]. The classical conf guration, with a short specimen placed between long input and output bars, used to perform compression test, can be modif ed for the study of dynamic mechanical behavior in tension and torsion test [2]. Even with a SHPB facility, several factors inf uence the accuracy of the results, including impedance mismatch, friction, specimen size effects, wave dispersion, stress equilibrium, among others. In this context, data processing is a key feature. This paper aims specif cally at adressing the relevant model issue for processing three-point bend test with SHPB. The paper f rst presents the experimental set-up. The different relevant model for analysing the data are then discussed. Finally, a test with a concrete specimen is fully analysed with the different models and the obtained results are compared.

2 HOPKINSON THREE-BAR/THREE-POINT BENDING TEST

The modif ed SHPB apparatus for dynamic bending used in this study has been proposed by [3]. A scheme of the set-up used in the present study is shown in Figure 1. The two transmission bars were used to support the specimen, and the load was applied via the incident bar.
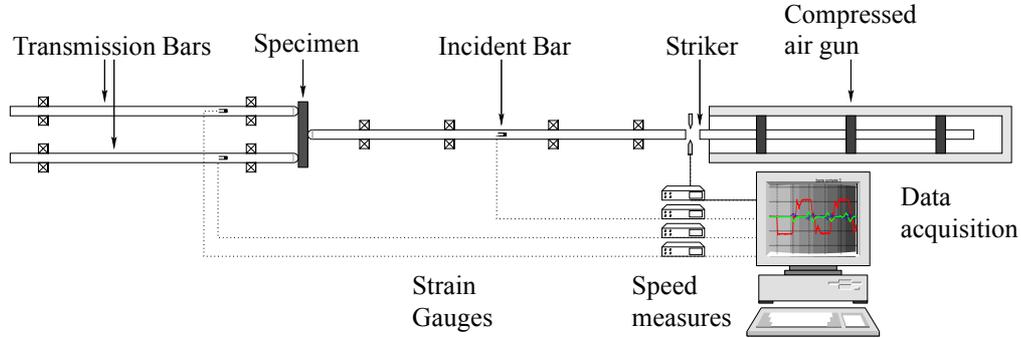

Figure 1. SHPB bending test set-up

The strain waves in the bars are measured using resistance gauges. The impact velocity is measured via photoelectric cells. The main advantage of SHPB is that it can be used to apply a dynamic load to a specimen and to measure both the *force* and the *velocity* at the impact point between the incident bar and the test specimen. The impact velocity and force are determined using the following classical formulae:

$$V_e(t) = -C_B \left(\varepsilon_i(t) - \varepsilon_r(t) \right) \tag{1}$$

$$F_e(t) = -Z_B \, C_B \left(\varepsilon_i(t) + \varepsilon_r(t) \right) \tag{2}$$

where $C_B = \sqrt{E_B / \rho_B}$ is the wave speed and $Z_B = E_B \, A_B / C_B$ the characteristic impedance. ε_i and ε_r are the incident and the ref ected waves at the input bar/specimen interface.

However, special precautions are required for processing raw data. The strain gage, glued in the middle of the long incident bar (Figure 1), records successively an incident and a ref ected wave. It is necessary to be able to perform highly precise time shifting procedures to transport the recorded pulses towards the specimen/bar interfaces. Indeed, a synchronization based on a simple alignment of the peaks of the pulses does not yield the correct time delay [4], [5].

3 MODELS FOR BENDING TEST INTERPRETATION

SHPB dynamic tests differ from quasi-static ones in the sense that neither a controlled force nor a displacement are imposed. The loading results from dynamic interactions between the deformed specimen and the incident bar at contact zone. The relation between the incident and ref ected waves (equations (1) and (2)) is linked to the relation between V_e and F_e. In the case of compression tests this relation can be written:

$$\varepsilon_r(t) = \frac{Z_C - Z_B}{Z_B + Z_C} \, \varepsilon_i(t) \quad \text{where} \quad Z_C = S \sqrt{\rho \, E} \quad \text{and} \quad Z_B = S_B \sqrt{\rho_B \, E_B} \tag{3}$$

The ref ected wave is concomitant and proportional to the incident wave. The elastic simulation is used to verify the slope of the ref ected wave and determine the start time of the transmitted wave [4]. In bending tests, the elastic response of the test specimen viewed as a *structure*, which relates V_e to F_e, determines the ref ection of the compression wave and hence the loading conditions. The accuracy of calculated intrinsic characteristics such as the tensile strength of the material, depends mainly on the level of realism of the specimen model used. Four models are presented below, along with the corresponding coupling equations.

3.1 Simply supported beam in a quasi-static state

Considering a simply supported beam in a quasi-static state, the bending moment in the central cross-section is:

$$M = \frac{F_e\,L}{4} \quad \text{where } L \text{ denotes the distance between the supports} \tag{4}$$

The relation between the force and the displacement at the end of the incident bar is:

$$U_e = \frac{F_e}{k_e} \quad \text{where} \quad k_e = \frac{48\,E\,I}{L^3} \tag{5}$$

The relation between the incident and ref ected waves is given by the convolution integral:

$$\varepsilon_r(t) = \varepsilon_i(t) - \int_0^t 2\,\varepsilon_i(\tau)\left(\delta(t-\tau) - \frac{1}{\tau_s}\,e^{-\frac{t-\tau}{\tau_s}}\right) d\tau \quad \text{where} \quad \tau_s = \frac{Z_B}{k_e} \tag{6}$$

3.2 Beam modelised by a single degree of freedom (SDOF) model

The previous model is improved by taking the inertial forces into account. The beam response is approximated via a single degree of freedom (SDOF) system, assuming the shape of the dynamically deformed beam to be similar to that of the quasi-static deformed beam.

$$m_e\,\ddot{U}_e + k_e\,U_e = F_e \quad \text{where} \quad m_e = \frac{17}{35}\,\rho\,S\,L \tag{7}$$

The coupling relation, at the center of the beam, between the force and the displacement is:

$$U_e(t) = \frac{1}{m_e\,\omega_e}\int_0^t F_e(\tau)\,sin(\omega_e(t-\tau))\,d\tau \quad \text{where} \quad \omega_e = \sqrt{\frac{k_e}{m_e}} \tag{8}$$

The relation between the incident and ref ected waves is given by the convolution integral:

$$\varepsilon_r(t) = \varepsilon_i(t) - \int_0^t \frac{2\,\varepsilon_i(\tau)}{\tau_e}\,e^{-\frac{t-\tau}{2\tau_e}}\left(cosh\left(\frac{(t-\tau)}{2\tau_e}\sqrt{\frac{\tau_s-4\tau_e}{\tau_s}}\right) - \sqrt{\frac{\tau_s}{\tau_s-4\tau_e}}\,sinh\left(\frac{(t-\tau)}{2\tau_e}\sqrt{\frac{\tau_s-4\tau_e}{\tau_s}}\right)\right)d\tau \tag{9}$$

$$\text{where} \quad \tau_e = \frac{m_e}{Z_B}$$

3.3 Modal superposition model

The motion of the beam is described in this model by superposing vibration modes. The coupling relation imposed at the center of the beam between the force and the displacement is the sum of convolution integrals :

$$U_e(t) = \sum_{j=1}^{\infty}\frac{1}{m_j\,\omega_j}\int_0^t F_e(\tau)\,sin(\omega_j(t-\tau))\,d\tau \tag{10}$$

where ω_j and m_j are respectively a vibration pulsation and the modal mass associated to a simply supported beam.
The relation between the incident and ref ected waves can be expressed as:

$$\varepsilon_r(t) = \varepsilon_i(t) - 2\int_0^t \varepsilon_i(\tau)\,\mathscr{L}^{-1}\left\{\frac{\overline{B}(s)}{\tau_m + \overline{B}(s)}\right\}\left(t-\tau\right)d\tau \tag{11}$$

where $\overline{B} = \sum_{j=1}^{\infty}\frac{s}{s^2+\omega_j^2}$ and $\tau_m = \frac{m_j}{Z_B}$ and $\mathscr{L}^{-1}$ denotes the inverse Laplace transform.

3.4 Semi-infinite beam model (SIBM)

During the first times of the impact, the stress wave does not reach the supports and *the situation is equivalent to a one-point bending test*. Therefore, in order to make the best possible use of the experimental data during the beginning of the test, it is proposed to consider a semi-infinite elastic beam. Using the time Laplace transform, the transient dynamic elastic response of the test specimen can be expressed in terms of the velocity V_e and of the force F_e:

$$w(x,t) = \int_0^t G_1(t-\tau)\, \Omega_1(x,\tau)\, d\tau - \int_0^t \Big(G_1(t-\tau) + G_2(t-\tau) \Big)\, \Omega_2(x,\tau)\, d\tau \qquad (12)$$

$$\text{where} \quad G_1(t) = \int_0^t \frac{V_e(\tau)}{\sqrt{\pi\,(t-\tau)}}\, d\tau \quad , \quad G_2(t) = \int_0^t \frac{F_e(\tau)}{4\,E\,I\,\alpha^3}\, d\tau \quad \text{with} \quad \alpha^4 = \frac{\rho\,S}{4\,E\,I} \qquad (13)$$

$$\text{and} \quad \Omega_1(x,t) = \frac{1}{\sqrt{\pi\,t}}\, \cos\!\left(\frac{\alpha^2\,x^2}{2\,t}\right) \quad , \quad \Omega_2(x,t) = \frac{1}{\sqrt{\pi\,t}}\, \sin\!\left(\frac{\alpha^2\,x^2}{2\,t}\right) \qquad (14)$$

Since the behavior of specimen is supposed to be elastic, the rotation at the origin remains zero. We obtain the following relation for the coupling imposed at the end of the incident bar between the force and the velocity during the first times:

$$V_e(t) = \frac{1}{2\,\eta} \int_0^t \frac{F_e(\tau)}{\sqrt{\pi\,(t-\tau)}}\, d\tau \quad \text{where} \quad \eta = 4\,E\,I\,\alpha^3 \qquad (15)$$

With the use of (1) and (2), we get the relation between the incident and reflected waves:

$$\varepsilon_r(t) = \varepsilon_i(t) - \int_0^t \frac{2\,\varepsilon_i(\tau)}{\sqrt{\tau_f}} \left(\frac{1}{\sqrt{\pi\,(t-\tau)}} - \frac{1}{\sqrt{\tau_f}}\, e^{\frac{t-\tau}{\tau_f}}\, erfc\!\left(\sqrt{\frac{t-\tau}{\tau_f}}\right) \right) d\tau \qquad (16)$$

Where $\tau_f = \left(\frac{2\eta}{Z_B}\right)^2$ and $erfc(t) = \frac{2}{\sqrt{\pi}} \int_t^\infty e^{-t^2}\, dt$ denotes the complementary error function.

4   EXPERIMENTAL SET-UP

Experimental tests are carried out with bars made of aluminium. The characteristics of the bars are specified in table 1. The specimen are unnotched micro-concrete beam with nominal length $L = 14\,cm$, a square cross-section $S = 16\,cm^2$, a density $\rho = 2000\,kg\,m^{-3}$ and a Young modulus $E = 12\,GPa$. An example of the raw signals recorded is presented in Figure 2.

Length of the striker	$L_I = 1.25\,m$
Length of the incident bar	$L_B = 3\,m$
Diameter of the bars	$\phi_B = 40 \times 10^{-3} m$
Bars cross-section	$S_B = 12.57 \times 10^{-4} m^2$
Young's modulus	$E_B = 74\,GPa$
Density	$\rho_B = 2800\,kg\,m^{-3}$
Elastic waves celerity	$C_B = 5140\,m\,s^{-1}$
Impedance	$Z_B = 18094\,kg\,s^{-1}$

Table 1: Characteristics of the SHPB system
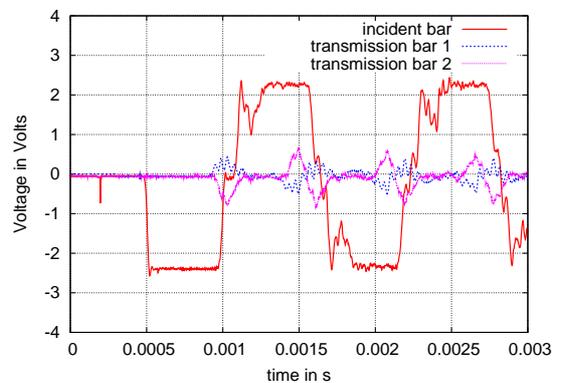
Figure 2. Raw signals measured

5 PROCESSING THE RAW SIGNALS USING VARIOUS MODELS

5.1 Time-shifting procedure

The recorded strain histories must f rst be shifted in time. In a f rst step, from the experimental incident wave, we evaluate elastic ref ected waves from the different models (Figure 3). In a second step, we use these simulated ref ected waves as reference to translate the recorded ref ected wave (Figure 4). The velocity V_e and the impact force F_e can now be deduced from the fundamental relations (1) and (2) (Figure 5 to 8).
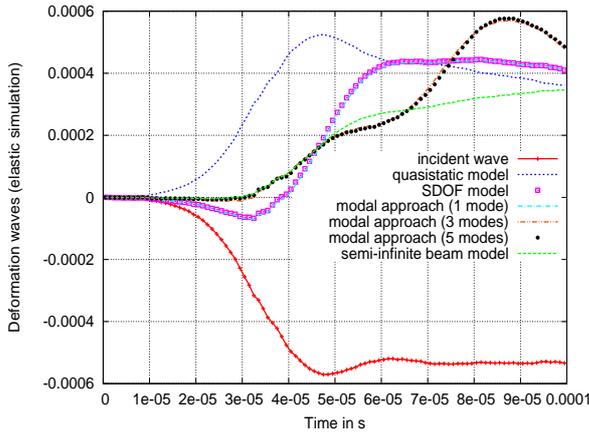
Figure 3: Experimental incident wave and simulated ref ected waves
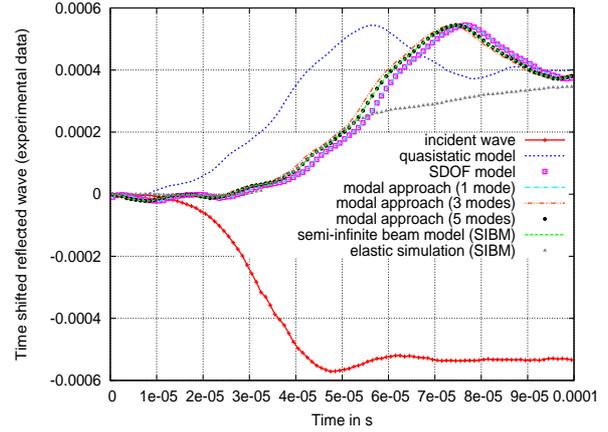
Figure 4: Experimental incident wave and time shifted experimental ref ected waves
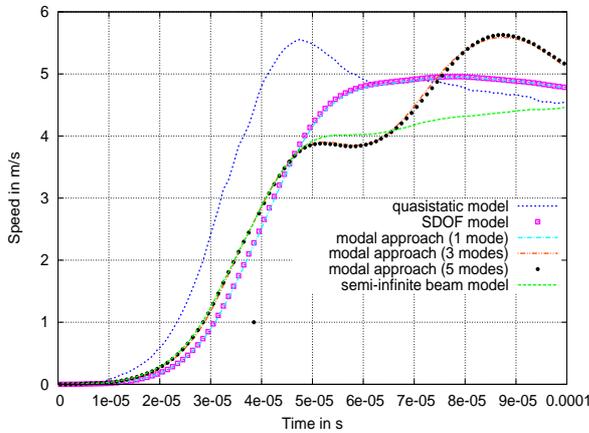
Figure 5: Impact speed V_e estimated by using the incident experimental wave and the simulated ref ected waves
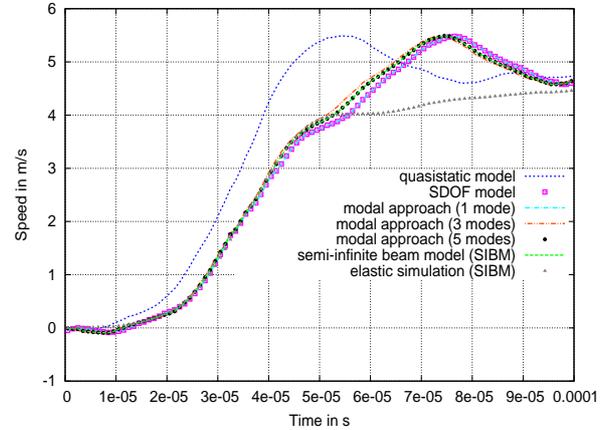
Figure 6: Impact speed V_e estimated by using the incident experimental wave and the time shifted experimental ref ected waves

5.2 Tensile strength

During the dynamic bending process, the stress state is not homogeneous. Consequently, the maximum tensile stress is obtained by performing a structural analysis. With the various models, the maximum stress can be expressed in terms of the displacement, in terms of the force or in terms of the incident and ref ected waves as follows:

- in the case of the quasi-static beam model:

$$\sigma(t) = \frac{6\,a\,E}{L^2}\,U_e(t) = \frac{a\,L}{8\,I}\,F_e(t) = -\frac{a\,L\,S_B\,E_B}{8\,I}\left(\varepsilon_i(t) + \varepsilon_r(t)\right) \tag{17}$$
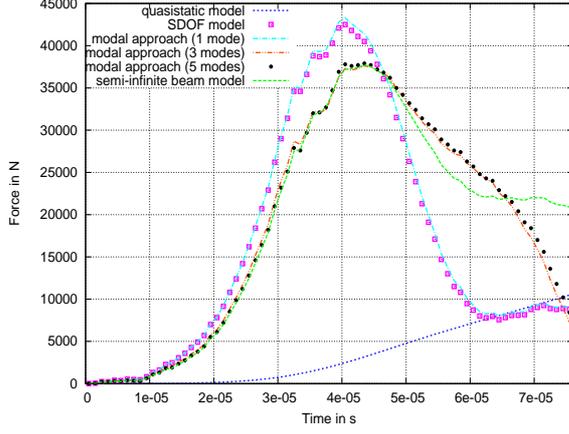
Figure 7: Impact forces F_e estimated by using the incident experimental wave and the simulated ref ected waves
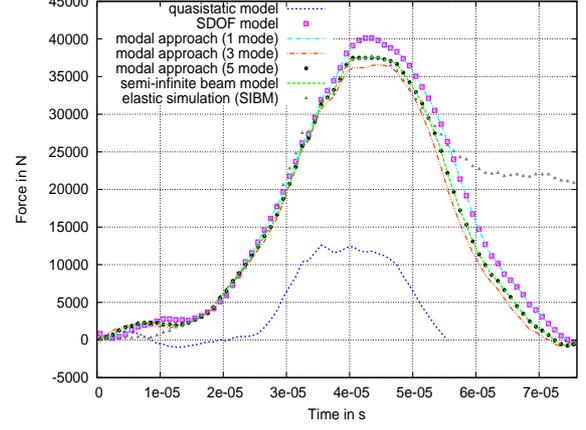

Figure 8: Impact forces F_e estimated by using the incident experimental wave and the time shifted experimental ref ected waves

- in the case of the SDOF beam model:

$$\sigma(t) = \frac{6\,a\,E}{L^2} U_e(t) == \frac{6\,a\,E\,C_B}{L^2} \int_0^t (\epsilon_r(\tau) - \epsilon_i(\tau))d\tau \tag{18}$$

- in the case of the modal analysis model:

$$\sigma(t) = \frac{a\,E\pi^2}{\rho S L^3} \sum_{n=1}^{+\infty} \frac{(2n-1)^2}{\omega_n} \int_0^t F_e(\tau)\sin(\omega_n(t-\tau))d\tau \tag{19}$$

- in the case of the semi-inf nite beam model:

$$\sigma(t) = a\,\alpha^2\,E\,V_e(t) = a\,\alpha^2\,E\,C_B\,(\varepsilon_r(t) - \varepsilon_i(t)) \tag{20}$$

The time evolution of the maximum stress is reported on Figures 9 and 10.
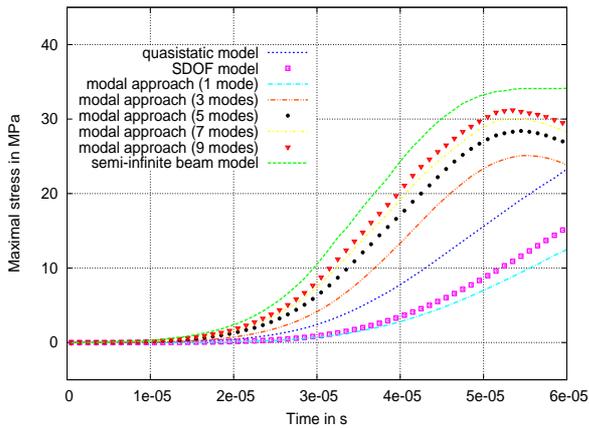
Figure 9: $\sigma(t)$ estimated using the incident experimental wave and the simulated ref ected waves.
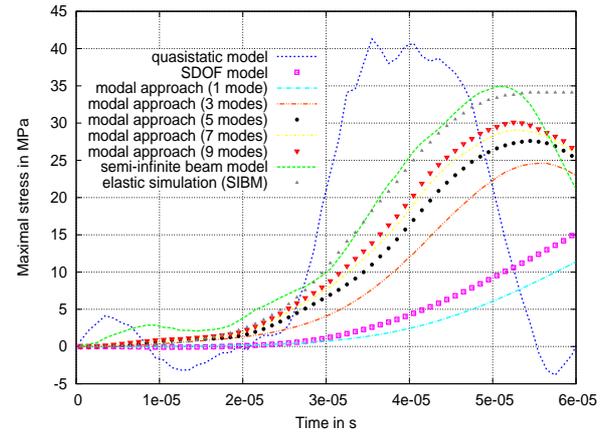
Figure 10: $\sigma(t)$ estimated using the incident experimental wave and the time shifted experimental ref ected waves

5.3 Strain rate

The strain rate is evaluated in the most highly strained f ber of the beam:
- in the case of the quasi-static beam or that of the SDOF beam, the strain rate is proportional to the velocity:

$$\dot{\varepsilon}(t) = \frac{6\,a}{L^2}\,V_e(t) \tag{21}$$

- in the case of the modal superposition model, the strain rate is given by:

$$\dot{\varepsilon}(t) = \frac{a\pi^2}{\rho S L^3}\sum_{n=1}^{+\infty}(2n-1)^2\int_0^t F_e(\tau)\cos(\omega_n(t-\tau))d\tau \tag{22}$$

- in the case of the semi-inf nite beam model, it is proportional to the acceleration:

$$\dot{\varepsilon}(t) = a\,\alpha^2\,\dot{V_e}(t) \tag{23}$$
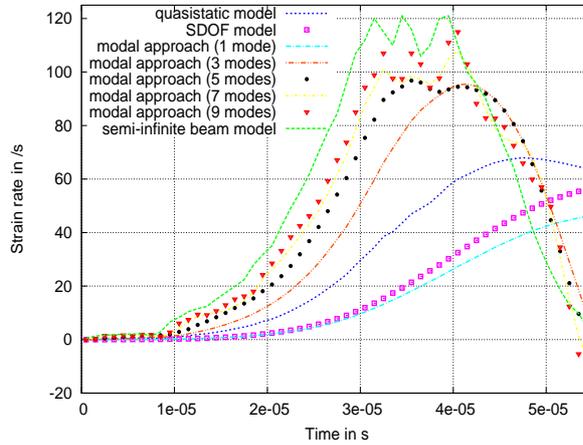
Figure 11: $\dot{\varepsilon}(t)$ estimated using the incident wave measured and ref ected waves obtained by the various elastic models.

6   RESULTS AND DISCUSSION

From the previous evaluations we can determine material dynamic characteristics (table 2). As expected, the dynamic tensile strength obtained is higher than the static one ($7\,MPa$). We observe a wide disparity in the estimated values for both the strain rate and the tensile strength. It seems that the modal analysis converges slowly, with an important number of modes to the same value as the semi-inf nite beam.

The results demonstrate that the choice of an analytical model for processing three-point bending test is not trivial. A key feature is the equivalence with a one-point bending test during the early stage of the impact, which must be taken into account for the time-shifting procedure.

Elastic model	Maximum impact force kN	Yield stress MPa	Strain rate s^{-1}
Quasi-static beam	12	40	68
SDOF	40	15	58
Modal analysis			
1 mode	40	12	46
3 modes	36	24.5	95
5 modes	37	27.5	98
7 modes	37	29	105
9 modes	37	30	110
Semi-inf nite beam	37	35	115

Table 2: Dynamic properties evaluated with various models.

ACKNOWLEDGMENTS

REFERENCES

[1] Field J. E., Walley S. M., Proud W. G., Goldrein H. T., Siviour C. R. (2004), Review of experimental techniques for high rate deformation and shock studies, *International Journal of Impact Engineering*, **30**, pp.725–775.

[2] Gray III GT. (2000), Classic split Hopkinson pressure bar testing, ASM Handbook, vol. 8, Mechanical Testing and Evaluation, Materials Park, ASM International, pp. 462–476.

[3] Yokoyama T., Kishida K. (1989) A novel impact three-point bend test method for determining dynamic fracture-initiation toughness. *Experimental Mechanics*, **29** (2), pp.188–194.

[4] Zhao H., Gary G. (1996), On the use of SHPB techniques to determine the dynamic behavior of materials in the range of small strains. *International Journal of Solids and Structures*, **33** (22), pp. 3363–3375.

[5] Mohr D., Gary G., Lundberg B. (2010), Evaluation of stress-strain curve estimates in dynamic experiments, *International Journal of Impact Engineering*, **37** (2), pp. 161–169